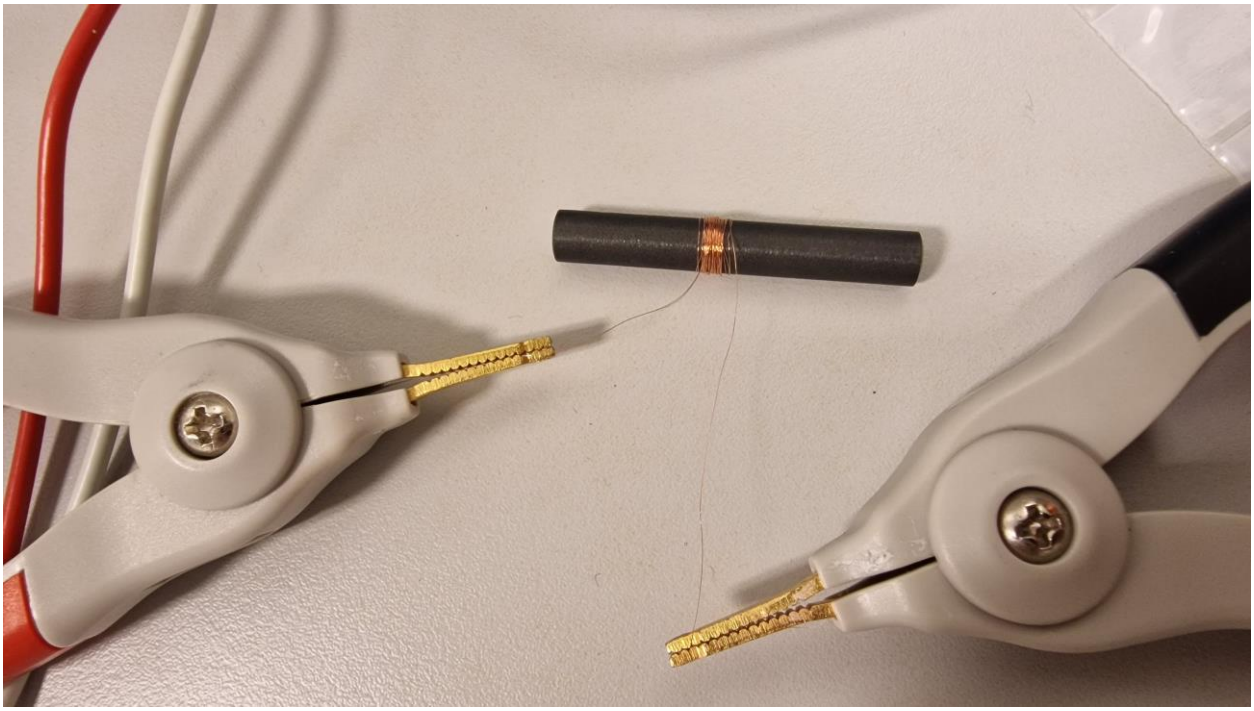

Theoretical and experimental analysis of inductor characteristics for hearing implants

Teoretisk och experimentell analys av induktoregenskaper för hörselimplantat

Christian Asadour
Abdulrahman Safi

DEPARTMENT OF ELECTRICAL ENGINEERING

CHALMERS UNIVERSITY OF TECHNOLOGY
Gothenburg, Sweden 2026
www.chalmers.se

BACHELORS THESIS IN BACHELOR OF SCIENCE PROGRAM
ELECTRICAL ENGINEERING

CHALMERS
UNIVERSITY OF TECHNOLOGY

Department of Electrical Engineering
CHALMERS University of Technology
Gothenburg, Sweden 2026

Theoretical and experimental analysis of inductor characteristics for hearing implants

Teoretisk och experimentell analys av induktoregenskaper för hörselimplantat

CHRISTIAN ASADOUR

ABDULRAHMAN SAFI

Examiner and Supervisor at Chalmers: Karl Johan Fredén Jansson

Industry Supervisor at Oticon Medical: Johannes Kocher

Department of Electrical Engineering
Chalmers University of Technology
SE-412 96 Gothenburg
Sweden
Telephone: +46 (0)31-772 1000

Cover: Photograph of a hand-wound prototype inductor on a ferrite rod, mounted between the kelvin clip probes of a precision LCR meter during measurements at Oticon Medical.

Gothenburg, Sweden 2026

Acknowledgements

This bachelor's thesis was carried out at the Department of Electrical Engineering at Chalmers University of Technology during the spring semester of 2026, in collaboration with Oticon Medical, as a part of the Bachelor of Science Program in Electrical Engineering.

We would like to express our sincere gratitude to Johannes Kocher, Director of Transducer & Electronics at Oticon Medical, for proposing this project and for his valuable guidance and support throughout the work. We would also like to thank the experienced engineers at Oticon Medical who assisted us in the laboratory during the prototype construction and measurement sessions; their practical know-how was essential to obtaining the experimental results presented in this report.

We would also like to thank Karl-Johan Fredén Jansson, our examiner at Chalmers University of Technology, for his academic guidance, constructive feedback and continuous support throughout the thesis process.

Finally, we would like to thank Oticon Medical for giving us the opportunity to carry out this project in a professional and inspiring environment, and for providing access to the laboratory, the materials, and the precision measurement equipment.

Christian Asadour and Abdulrahman Safi, Gothenburg 2026

Abstract

Implantable hearing devices rely on inductive coils to transfer power and signals wirelessly across the skin. The electrical and magnetic properties of these coils directly affect device efficiency, and size. This thesis investigates how core material, core diameter, wire diameter, and number of turns affect the inductance, DC resistance, quality factor, magnetic flux, and physical size of wire-wound inductors intended for hearing implant applications. The work was carried out in collaboration with Oticon Medical.

A MATLAB model was implemented and evaluated for five core materials across seven core diameters and two wire diameters at a target inductance of 100 μH. Four prototype coils were also hand-wound on ferrite rod cores at Oticon Medical's laboratory and measured using a Sourcetronic ST2827A precision LCR meter. The theoretical results were compared with the experimental measurements to evaluate how well the model reflected practical coil behavior.

The findings provide a comparative framework for understanding how material and geometric choices affect coil performance and highlight key considerations for future coil design in implantable hearing devices.

Table of Contents

Abbreviations

AC = Alternating current

ACR = AC Resistance

DC = Direct current

DCR = DC Resistance

μH = Micro henry

nF = Nano farad

Ω = Ohm

LC = Inductor-Capacitor

Q = Quality factor

1. Introduction

Implantable hearing devices are sophisticated medical systems designed to restore or enhance auditory perception in patients with moderate to profound hearing loss [1], [2]. These systems integrate electronic circuits, magnetic components, and biocompatible materials to interact with the auditory system safely and effectively. By directly stimulating the cochlea or auditory nerve, these devices can bypass damaged regions of the ear, providing improved hearing outcomes compared to conventional hearing aids [2]. A key challenge in the design of such devices is achieving high electromagnetic performance while ensuring reliable electrical behavior, as small deviations in coil parameters can significantly affect signal transfer and overall device function [3].

This thesis focuses on the electrical and electromagnetic analysis of inductive components used in implantable hearing devices. Specifically, it investigates how design parameters, including core material, core size, and wire size, affect critical coil properties such as inductance, DC resistance, quality factor, and magnetic flux. Understanding these relationships is essential to optimize coil performance within the limited volume available in implantable devices [4]. The results are intended to provide comparative data for Oticon Medical, supporting design decisions for future implantable devices by highlighting the influence of material and geometric choices on coil behavior.

1.1 Background

This study was carried out in collaboration with Oticon Medical, a global company specializing in implantable hearing solutions dedicated to bringing the benefits of sound to people at every stage of life [5]. Inductive components are widely used in electronics for purposes such as filtering, impedance matching, energy transfer, and signal processing, where precise inductance and low resistance are critical [6]. In implantable hearing devices, coils must achieve high inductance in a limited volume, maintain low resistance to minimize power loss, and operate reliably under variable environmental conditions [3], [4].

Ferrite cores are commonly employed in such coils due to their high relative permeability, which increases magnetic coupling and enables higher inductance within small form factors [7]. The choice of ferrite material, core size, and geometry directly impacts the coil's performance in LC circuits used for power transfer or signal transduction [8]. However, variations in material properties or construction tolerances can introduce deviations from theoretical predictions, emphasizing the need for both experimental validation and careful design [6].

By comparing coils with varying materials, core diameters, and wire sizes, this thesis aims to generate systematic knowledge on how these parameters influence electrical and magnetic behavior. These insights provide a technical basis for future evaluation, prototyping, and design decisions for implantable hearing devices, ensuring that performance specifications can be met reliably within the physical constraints of the device.

1.2 Aim

The primary aim of this thesis is to investigate how core material, core size, and wire size affect the electrical and magnetic performance of coils for implantable hearing devices.

Key objectives include:

- Comparing different coil configurations to evaluate trends in inductance, resistance, quality factor, and magnetic flux.

- Determining how coil parameters influence LC circuit behavior.
- Providing comparative data to support Oticon Medical in making technical design decisions.

The work does not aim to develop a final coil design, but rather to provide a clear comparative framework for understanding design impacts.

1.3 Scope and limitations

This thesis focuses on the component-level and circuit-level behavior of selected coil configurations. It does not include:

- Final coil optimization or clinical validation.
- Biological or mechanical analysis, packaging, sterilization, or long-term biocompatibility studies.

The analysis is limited to how variations in core material, size, and wire diameter influence electrical parameters and magnetic flux. LC circuit behavior is studied as an example of functional impact, but full system performance is outside the scope.

1.4 Research questions

The study addresses the following questions:

- How do core material, core size, and wire size affect coil parameters such as inductance, DC resistance, quality factor, and magnetic flux?
- What trends can be observed when comparing different coil configurations through theoretical calculations and experimental testing?
- How do the investigated coil parameters influence LC circuit performance?
- How can these results be used as a technical basis for future evaluation and decision-making in implantable hearing device development?

2. Theoretical background

This chapter provides the fundamental scientific concepts required to understand the principles of inductors and LC resonant circuits. It is intended for readers with a background in electrical engineering and focuses solely on scientific explanations without reference to specific projects or material parameters. The chapter first describes the human auditory system, then the principles of inductive energy storage, and finally the behavior of LC circuits.

2.1 Physiology of hearing

The human ear is the organ responsible for hearing and maintaining balance. It consists of three main regions: the outer ear, the middle ear, and the inner ear. The outer ear, composed of the pinna and ear canal, collects and funnels sound waves from the environment toward the eardrum. The middle ear contains the eardrum and the ossicles the malleus, incus, and stapes which transmit mechanical vibrations to the inner ear. In the inner ear, the cochlea converts these vibrations into electrical signals that are sent to the brain via the auditory nerve [1]. The brain interprets these signals as sound, allowing for perception of pitch, volume, and spatial location.
Damage or dysfunction in any part of this auditory pathway can result in impaired hearing, ranging from mild loss to complete deafness [2]. Understanding this physiology is essential for the design of devices that interact with the auditory system, as it defines the frequency ranges and signal characteristics that must be supported.

2.2 Principles of inductive energy transfer

Inductors are passive components that store energy in magnetic fields when an electric current flows through a conductor. This property allows them to transfer energy and signals via magnetic coupling, which is widely utilized in both industrial and biomedical applications. Inductive links rely on two coils in proximity: when current flows through the primary coil, a magnetic field is created that induces a current in the secondary coil. This principle enables wireless transfer of energy and data, even through barriers such as the skin [3].
Efficient energy transfer requires that the inductor stores energy effectively and dissipates minimal energy as heat. The geometry of the coil, including the number of turns, the spacing between turns, and the shape of the wire, plays a critical role in the coil's performance. A well-designed coil balances compactness with the ability to store energy, which is especially important in applications where space is limited [4].

2.3 The inductor

An inductor, typically realized as a wire-wound coil, has four key characteristics: inductance, resistance, quality factor, and magnetic flux.

2.3.1 Inductance

Inductance measures the ability of a coil to store energy in its magnetic field. The strength of this storage depends on the coil's geometry and the properties of any core material used. Increasing the number of turns or employing a material that enhances the magnetic field can increase inductance [6]. High inductance allows more energy to be stored, which is beneficial for efficient signal transfer and resonance.

2.3.2 Resistance

All conductors exhibit some electrical resistance, which converts part of the energy in the circuit into heat. In a coil, this resistance, known as DC resistance, is determined by the wire's length, cross-sectional area, and the inherent conductivity of the material [6]. Lower resistance is generally preferred to reduce energy loss, especially in applications that require high efficiency or minimal heating near sensitive environments.

2.3.3 Skin and proximity effects

At low frequencies, current flows uniformly through the conductor. At higher frequencies, however, current tends to concentrate near the surface of the conductor due to the skin effect, and interactions between adjacent turns can further distort the current distribution, known as the proximity effect [8]. In low-frequency applications, such as audio and biomedical systems, these effects are minimal, and the AC resistance of the coil is essentially equal to its DC resistance.

2.3.4 Quality factor

The quality factor, or Q, quantifies how effectively a coil stores energy relative to the energy it dissipates per cycle. A high Q indicates efficient energy storage and low losses, while a low Q reflects higher dissipation. The Q of a coil is influenced by its inductance, resistance, and the frequency at which it operates [8]. High-Q coils are desirable in applications where resonance and selective frequency response are required.

2.3.5 Magnetic flux

Magnetic flux represents the total magnetic field passing through a given area of the coil. The magnetic flux is directly related to the current flowing through the coil and the number of turns [6]. Changes in magnetic flux induce voltage in nearby conductors, enabling wireless energy transfer and signal induction. The flux characteristics are fundamental to the coil's performance in resonant circuits.

2.4 Capacitors in LC circuits

Capacitors store energy in an electric field between their plates. When combined with an inductor, the capacitor forms an LC circuit, which can resonate at a particular frequency [7]. The capacitor and inductor continuously exchange energy between their electric and magnetic fields, creating oscillations at the circuit's natural resonant frequency. The interaction between the inductor and capacitor defines the resonance characteristics and the energy transfer efficiency of the circuit.

2.5 Resonance in LC circuits

Resonance occurs when the reactive effects of the inductor and capacitor cancel each other out. At this frequency, the circuit can oscillate with minimal energy loss, and the amplitude of voltage and current can reach a peak [7]. The sharpness of the resonance, often described by the quality factor, indicates how selective the circuit is to a particular frequency [8]. In practical applications, designing for resonance ensures efficient energy transfer, precise frequency response, and minimal losses.

2.6 Applications and considerations

LC circuits and inductors are widely used in filtering, signal processing, wireless power transfer, and sensing applications [3], [4]. Proper design requires consideration of the geometry and size of the coil and capacitor, energy storage efficiency and loss minimization, frequency characteristics and resonance tuning, and physical constraints and environmental effects such as temperature and proximity to other conductive materials [6]. Understanding these fundamental principles is essential for any system that relies on inductive energy storage or resonance phenomena.

3. Method

This chapter describes the method used in the project. The work was divided into several stages to create a structured process for comparing how different core materials, core sizes, and wire diameters affect coil performance. The stages were: material investigation, theoretical calculations, concept selection, prototype construction, experimental testing, and evaluation.

3.1 Material investigation

The first step was to investigate possible core materials and coil configurations. The materials were evaluated based on magnetic permeability, electrical properties, availability, and suitability for compact coil designs.

3.2 Theoretical calculations

Theoretical calculations were performed to estimate the expected performance of the selected materials and coil configurations. Calculations included inductance, number of turns, wire length, DC resistance, quality factor, and magnetic flux. Different combinations of core material, core size, and wire diameter were compared to identify trends and promising designs.

3.3 Concept selection

Based on the theoretical results, coil concepts were selected for further development. Available materials and components in the lab or office were reviewed, and additional items were ordered as needed to enable the construction of the coils. The selected concepts represented different combinations of material, size, and wire diameter, focusing on representative designs rather than fully optimized final coils.

3.4 Prototype construction

The chosen coils were constructed manually by winding enameled copper wire around the selected core materials. The number of turns, wire diameter, and core dimensions were based on the theoretical calculations. The winding procedure was kept as consistent as possible to reduce variations between prototypes.

3.5 Experimental testing

The constructed coils were tested to measure inductance and DC resistance. The experimental results were compared with the theoretical predictions to evaluate the agreement between the MATLAB model and the practical coils.

3.6 Evaluation and conclusion

The theoretical and experimental results were compiled in tables and graphs. These results were then used as the basis for the discussion, conclusions, and provided guidance for future coil design in implantable hearing devices.

4. Formulas

This chapter presents the formulas used in the calculations. The equations are later used in Chapter 5 to implement the MATLAB calculations.

Core and wire cross-sectional area

The cross-sectional area of a circular core or wire can be calculated as:

$$A = \pi \times r^2 \tag{4.1}$$

Where:
A = Cross-sectional area $[m^2]$
r = Radius $[m\ ]$

The radius is terms of diameter can be calculated as:

$$r = \frac{d}{2} \tag{4.2}$$

Where:
r = Radius [m]

Inductance

The inductance of a solenoid can be calculated as [6]:

$$L = \frac{\mu \times N^2 \times A}{l} \tag{4.3}$$

Where:
L = Inductance $[H\ ]$
μ = Absolute permeability $[H/m]$
N = Number of turns in the coil
A = Area of the coil core $[m^2]$
l = Length of the coil $[m\ ]$

The permeability of the material is calculated as [6]:

$$\mu = \mu_0 \times \mu_r \tag{4.4}$$

Where:
μ = Absolute permeability $[H/m]$
μ_0 = Permeability of free space $[4\pi \times 10^{-7}\ H/m]$
μ_r = Relative permeability of the core material

Number of turns

By rearranging the inductance formula, the required number of turns can be calculated as:

$$N = \sqrt{\frac{L \times l}{\mu \times A}} \tag{4.5}$$

Where:
N = Number of turns
L = Target inductance [H]
l = Coil length [m]
μ = Absolute permeability [H/m]
A = Core cross-sectional area [m^2]

Wire length

The total wire length is estimated from the number of turns and the core circumference:

$$l_{wire} = \sum_{k=1}^{N_{layers}} n_k \times \pi \times (D_{core} + (2k-1)D_{wire}) \tag{4.6}$$

Where:
l_{wire}= Total wire length [m]
k = Layer index
n_k = Number of turns in layer k
N_{layers} = Total number of winding layers
D_{core} = Core diameter [m]
D_{wire} = Wire diameter [m]

DC Resistance

The DC resistance of the copper wire is calculated as [6]:

$$R_{DC} = \rho \times \frac{l}{A} \tag{4.7}$$

Where:
R_{DC} = DC resistance [Ω]
ρ = Resistivity of the wire material [$\Omega \times m$]
l = Length of the wire [m]
A = Area of the wire [m^2]

Skin depth

The skin depth is calculated as [6]:

$$\delta = \sqrt{\frac{2\rho}{2 \times \pi \times f \times \mu}} \tag{4.8}$$

Where:
δ = Skin depth [m]

ρ = Resistivity of the wire material [$\Omega \times m$]
f = Frequency [Hz]
μ = Absolute permeability [H/m]

AC Resistance

AC resistance accounts for the skin effect at high frequencies [8]:

$$R_{AC} = \begin{matrix} R_{DC}, & if\ \delta \gg r_{wire} \\ R_{DC} \times \frac{r_{wire}}{2\delta}, & if\ \delta \leq r_{wire} \end{matrix} \quad (4.9)$$

Where:
R_{AC} = AC Resistance [Ω]
r_{wire} = Wire radius [m]
R_{DC} = DC Resistance [Ω]

Quality factor

The quality factor is calculated as [8]:

$$Q = \frac{X_L}{R_{AC}} \quad (4.10)$$

Where X_L is the inductive reactance [6]:

$$X_L = 2 \times \pi \times f \times L \quad (4.11)$$

Where:
Q = Quality factor
X_L = Inductive reactance [Ω]
f = Frequency [Hz]
L = Inductance [H/m]
R_{AC} = Total resistance [Ω]

Magnetic flux

The magnetic flux can be calculated as [6]:

$$\Phi = B \times A \quad (4.12)$$

Where B is the magnetic flux density in the core:

$$B = \mu_r \times \mu_0 \times H \quad (4.13)$$

Where:
Φ = Magnetic flux [Wb]
B = Magnetic flux density [T]
A = Core area [m^2]
μ_0 = Permeability of free space [$4\pi \times 10^{-7}\ H/m$]
μ_r = Relative permeability of the core material
H = Magnetic field intensity

Number of winding layers

The number of turns per layer can be calculated as:

$$N_{layer} = \frac{l_{coil}}{D_{wire}} \quad (4.14)$$

The total number of layers can be calculated as:

$$N_{layers} = \left| \frac{N}{N_{layer}} \right| \quad (4.15)$$

Where:
N_{layer} = Turns per layer
N_{layers} = Total number of winding layers
l_{coil} = Coil length [m]
D_{wire} = Wire diameter [m]

Total coil diameter and area

The outer coil diameter can be calculated as:

$$D_{outer} = D_{core} + 2 \times N_{layers} \times D_{wire} \quad (4.16)$$

The outer coil radius can be calculated as:

$$R_{outer} = \frac{D_{outer}}{2} \quad (4.17)$$

Where:
D_{outer}= Outer coil diameter [m]
R_{outer}= Outer coil radius [m]
D_{core}= Core diameter [m]
N_{layers}= Total winding layers
D_{wire}= Wire diameter [m]

LC resonance frequency

The LC resonance frequency is calculated as [7]:

$$f_0 = \frac{1}{2\pi\sqrt{LC}} \quad (4.18)$$

Where:
f_0 = Resonance frequency [Hz]
L = Inductance [H]

C = Capacitance [F]

LC Q-factor

The LC quality factor can be calculated as [7]:

$$Q_{LC} = \frac{1}{R} \times \sqrt{\frac{L}{C}} \tag{4.19}$$

Where:
Q_{LC} = LC quality factor
R = Total series resistance in the LC circuit
L = Inductance [H]
C = Capacitance [F]

LC magnitude response

The magnitude response of the LC circuit can be calculated as [7]:

$$|H(F)| = \frac{1}{\sqrt{1+Q_{LC}^2\left(\frac{f}{f_0}-\frac{f_0}{f}\right)^2}} \tag{4.20}$$

Where:
$|H(F)|$ = Magnitude response
f_0 = Resonance frequency [Hz]
Q_{LC} = LC quality factor
f = Operating frequency [Hz]

Bandwidth

The bandwidth of the LC circuit can be calculated as [7]:

$$BW = f_2 - f_1 \tag{4.21}$$

BW = Bandwidth [Hz]
f_1 = Lower cutoff frequency [Hz]
f_2 = Upper cutoff frequency [Hz]

5. Implementation

This chapter describes how the theoretical calculations were implemented in MATLAB. The aim was to evaluate different coil configurations by varying core material, core diameter, and wire diameter. A fixed target inductance of 100 µH was used for all configurations.
For each configuration, MATLAB was used to calculate the number of turns, wire length, DC resistance, skin depth, AC resistance, inductive reactance, Q-factor, magnetic flux, and total coil area. The calculations were based on the formulas presented in Chapter 4. The results were organized into tables and visualized in graphs to facilitate comparison between different designs.

5.1 Calculation setup

The calculations were performed using both fixed and variable input parameters. The fixed parameters included the target inductance, coil length, frequency, and copper resistivity. These parameters were kept constant to allow comparison of the effects of changing core material, core diameter, and wire diameter.
The variable parameters were the core material, core diameter, and wire diameter. The core diameter varied from 2 mm to 8 mm. Two copper wire diameters were investigated: 0.15 mm and 0.07 mm.
The absolute permeability of each core material was calculated using the assigned relative permeability values and Equation (4.4). Calculations were repeated for every combination of core material, core diameter, and wire diameter to generate a complete dataset for comparison.

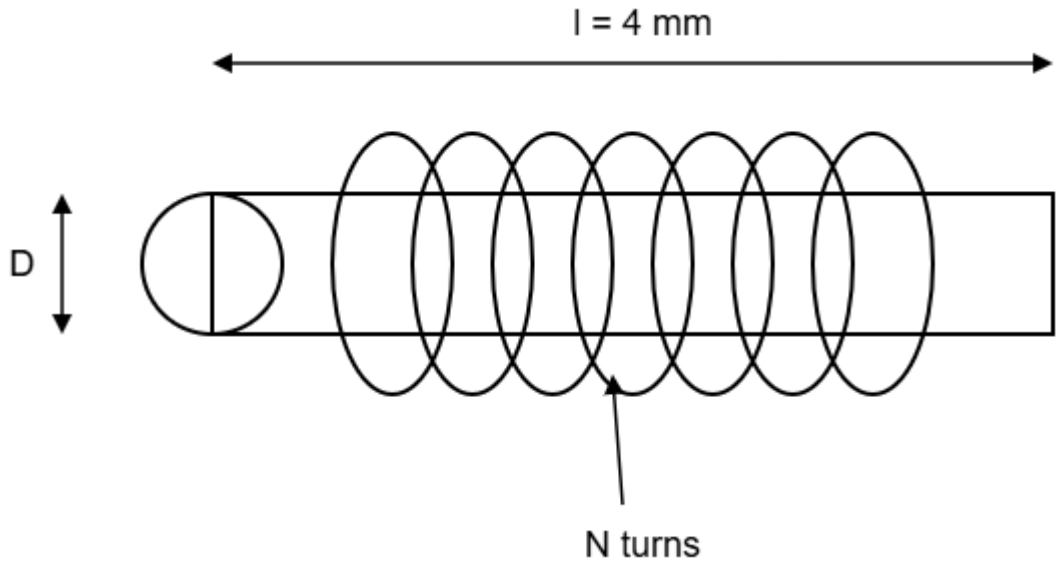

Figure 5.1: Simplified diagram of a solenoid coil showing the key geometric parameters: core diameter D, winding length l = 4 mm, and number of turns N.

5.1.1 Core materials

The first step in the calculations was to define the core materials. Each material was represented by its relative permeability, which was used to calculate the absolute permeability.
The selected materials were chosen to cover a wide range of magnetic properties. This allowed comparison of how material permeability influences the required number of turns, DC resistance, Q-factor, and magnetic flux.
The relative permeability values used in the calculations are presented in table 5.1.

Table 5.1: Relative permeability values for the selected core materials used in the calculations

Material	Relative permeability
Air	1
Iron	100
Ferrite nickel-zinc	500
Ferrite manganese-zinc	1500
Vacuflux 50	4000

5.1.2 Core and wire dimensions

The core diameter and wire diameter were varied to investigate how the physical dimensions of the coil affect the calculated performance. The core diameter varied from 2 mm to 8 mm. For each core diameter, the corresponding radius and cross-sectional area were calculated using Equations (4.1) and (4.2) presented in Chapter 4.

Two enameled copper wire diameters were investigated: 0.15 mm and 0.07 mm. The resistivity of copper was kept constant for both wire diameters.

Table 5.2: Core diameter and corresponding cross-sectional area

Core diameter [mm]	Core radius [mm]	Core area [mm²]
2	1	3.1416
3	1.5	7.069
4	2	12.566
5	2.5	19.635
6	3	28.274
7	3.5	38.485
8	4	50.27

Table 5.3: Wire specifications used in the calculations

Wire material	Resistivity [Ω•m]	Wire diameter [mm]	Wire area [mm²]
Enameled copper	1.678×10^{-8}	0.15	0.01767
Enameled copper	1.678×10^{-8}	0.07	0.00385
Silver	1.59×10^{-8}	-	-
Gold	2.44×10^{-8}	-	-

Silver and gold were included only as reference conductor materials. The calculations were based on enameled copper wire. However, silver and gold are relevant to mention because they are commonly used or considered in biomedical and implant related applications where electrical conductivity, material stability, and corrosion resistance are important. The comparison shows that silver has a slightly lower resistivity than copper, while gold has a higher resistivity.

5.2 Coil calculations

This section describes the theoretical calculations performed for the coils. The purpose is to detail how the coil geometry, material properties, and wire dimensions were used to calculate inductance, number of turns, resistance, and other coil parameters. All calculations presented here form the basis for the systematic evaluation performed in MATLAB in Section 5.3.
All coil configurations were designed with a target inductance of 100 μH.

5.2.1 Geometry calculations

The core and wire radius were calculated using Equation (4.2), and the corresponding cross-sectional areas were calculated using Equation (4.1). The core cross-sectional area was used for inductance and number of turns calculations, while the wire cross-sectional area was used for resistance calculations.

5.2.2 Permeability and number of turns

Relative permeability values were assigned to each core material. The absolute permeability was calculated using Equation (4.4). The number of turns required to achieve the target inductance was calculated using Equation (4.5).

5.2.3 Wire length and DC Resistance

The total wire length was calculated from the number of turns, layers and the core circumference using Equation (4.6). DC resistance was calculated using Equation (4.7) from the copper resistivity, wire length, and wire cross-sectional area.

5.2.4 Skin depth and AC Resistance

The skin depth was calculated using Equation (4.8). AC resistance was evaluated using Equation (4.9). If $\delta \gg r_{wire}$, AC resistance is approximately equal to DC resistance; otherwise, the resistance increases due to current crowding at the wire surface.

5.2.5 Inductive reactance and coil Q-factor

Inductive reactance was calculated using Equation (4.11). The coil Q-factor was calculated using Equation (4.10) based on inductive reactance and AC resistance.

5.2.6 Magnetic flux

In this part, the magnetic flux was not directly calculated as a numerical value. Instead, the relationship between magnetic flux, magnetic flux density, core area, and relative permeability was derived.

The starting point was the magnetic flux equation, shown in Equation (4.12):

The magnetic flux density in the core was expressed using Equation (4.13):

By substituting Equation (4.13) into Equation (4.12), the magnetic flux can be written as:

$$\Phi = \mu_r \mu_0 H \times A$$

The core cross-sectional area was assumed to be circular and was calculated using Equation (4.1), together with Equation (4.2) for the radius:

$$A = \pi \times r^2, r = \frac{d}{2}$$

Substituting the circular core area into the magnetic flux expression gives:

$$\Phi = \mu_r \mu_0 H \times \frac{\pi d^2}{4}$$

This relationship shows how the magnetic flux depends on the relative permeability of the core material and the core diameter. Since μ_0, H and $\frac{\pi}{4}$ are constant for the comparison, the relationship can be simplified to:

$$\Phi \sim \mu_r \times d$$

5.2.7 Total coil size

Number of turns per layer was calculated using Equation (4.14), the number of winding layers using Equation (4.15), and the outer diameter using Equation (4.16). The outer radius and total coil area were calculated using Equations (4.17) and (4.1).

5.2.8 LC resonance frequency

The LC resonance frequency was calculated using Equation (4.18):
with L = 100 μH and C = 200 nF, resulting in a resonance frequency of approximately 35.6 kHz.

5.2.9 LC magnitude response

The LC quality factor was first calculated using Equation (4.19), based on the total series resistance, inductance, and capacitance. The magnitude response of the LC circuit was then calculated using Equation (4.20) over a frequency range around the resonance frequency.

5.2.10 Bandwidth from the LC curve

Bandwidth was determined from the lower and upper cutoff frequencies where the normalized magnitude response dropped to 0.707 of its maximum value, based on Equation (4.20). The bandwidth was then calculated using Equation (4.21).

5.3 MATLAB

All coil calculations were loaded into MATLAB to make the process systematic, repeatable, and efficient. This approach allowed rapid evaluation of multiple coil configurations by simply changing input parameters such as wire diameter, core diameter, and relative permeability.

For each configuration, MATLAB automatically calculated:

- Number of turns
- Wire length
- DC resistance
- Skin depth
- AC resistance
- Inductive reactance
- Q-factor

- Total coil area
- Outer radius
- Outer diameter

The calculated values were saved in tables and later used to generate graphs. The graphs visually present how the parameters changed for different core diameters, core materials, and wire diameters. Separate tables and graphs were created for the two wire diameters (0.15 mm and 0.07 mm). These results are presented in Chapter 6.

5.4 Experimental coil construction and measurement

This section describes the material selection, coil construction process, and measurement method used for the experimental verification. The purpose of the experimental part was to build physical coils and compare the measured values with the theoretical calculations from MATLAB. This was done to evaluate how well the theoretical model matched the practical coil behavior.

5.4.1 Material selection

The experimental coils were built using two types of ferrite cores and enameled copper wire. The ferrite materials were chosen based on availability and the circumstances of the project. The first ferrite core had a relative permeability of 2300 and a diameter of 6 mm, and the second core had a relative permeability of 125 and a diameter of 4 mm.
None of the selected cores had the exact relative permeability used in the initial theoretical MATLAB calculations. Therefore, all calculations were repeated using the actual permeability values of the chosen cores, in order to determine the expected number of turns, inductance, and resistance for each coil.
Since the calculated number of turns was often non-integer (e.g., 3.28749 turns), the number of turns was rounded to the nearest whole number. This rounding is necessary because it is difficult, if not impossible, to wind a fractional turn by hand with precision. As a result, the practical coils are expected to display slightly different inductance values compared to the theoretical targets 100 μH.

Table 5.4 summarizes the planned coils, the recalculated theoretical values, and the practical constraints expected during construction.

Table 5.4: Planned ferrite-core coils with recalculated theoretical values and expected practical constraints.

Prototype	Core type	Relative permeability	Core diameter (mm)	Wire diameter (mm)	Planned number of turns	Expected inductance (μH)	Expected resistance (Ω)
A	Ferrite	2300	6	0.15	3	180	0.053128
B	Ferrite	2300	6	0.07	3	180	0.24395
C	Ferrite	125	4	0.15	14	97-98	0.16815
D	Ferrite	125	4	0.07	14	97-98	0.77214

In addition to the hand-wound ferrite cores, two ready-made coils were ordered, and one existing coil from Oticon was used as a reference. The Oticon medical coil served as a reference for our calculations, allowing us to validate the MATLAB code and ensure consistency with an existing, known component. The two ready-made coils were included specifically to verify that the measurement setup functioned correctly before testing the hand-wound prototypes, providing

confidence in the experimental procedure and the accuracy of the results.

Table 5.5: Reference coil from Oticon Medical.

Coil	Core type	Relative permeability	Core diameter (mm)	Wire diameter (mm)	Number of turns	Inductance (µH)	Resistance max (Ω)
1	Air	1	3.4	0.15	170	110	3.5

Table 5.6: Pre-built coils for measurement verification.

Coil	Core type	Inductance (µH)	Resistance max(Ω)
1	Ferrite	10	1.8
2	Ceramic	0.1	0.28

5.4.2 Coil construction process

The experimental part of the work was performed at Oticon Medical's laboratory. The construction procedure for each prototype consisted of the following steps:

1. The appropriate length of enameled copper wire was cut.
2. The calculated number of turns was wound by hand around the ferrite rod core, taking care to keep the turns as evenly spaced and confined as possible to a short section in the middle of the rod.
3. The wound section was fixed in place using a UV-cured adhesive, exposed to ultraviolet light to harden rapidly.
4. The enamel insulation was removed from both wire ends using a temperature-controlled soldering iron with tin solder, leaving a small, well-tinned contact pad at each end.

(A) (B)

Figure 5.2: Images of the hand-wound ferrite core coils. (A) Prototype A, Relative permeability = 2300, 6 mm diameter, 0.15 mm wire. (B) Prototype B, Relative permeability = 2300, 6 mm diameter, 0.07 mm wire.

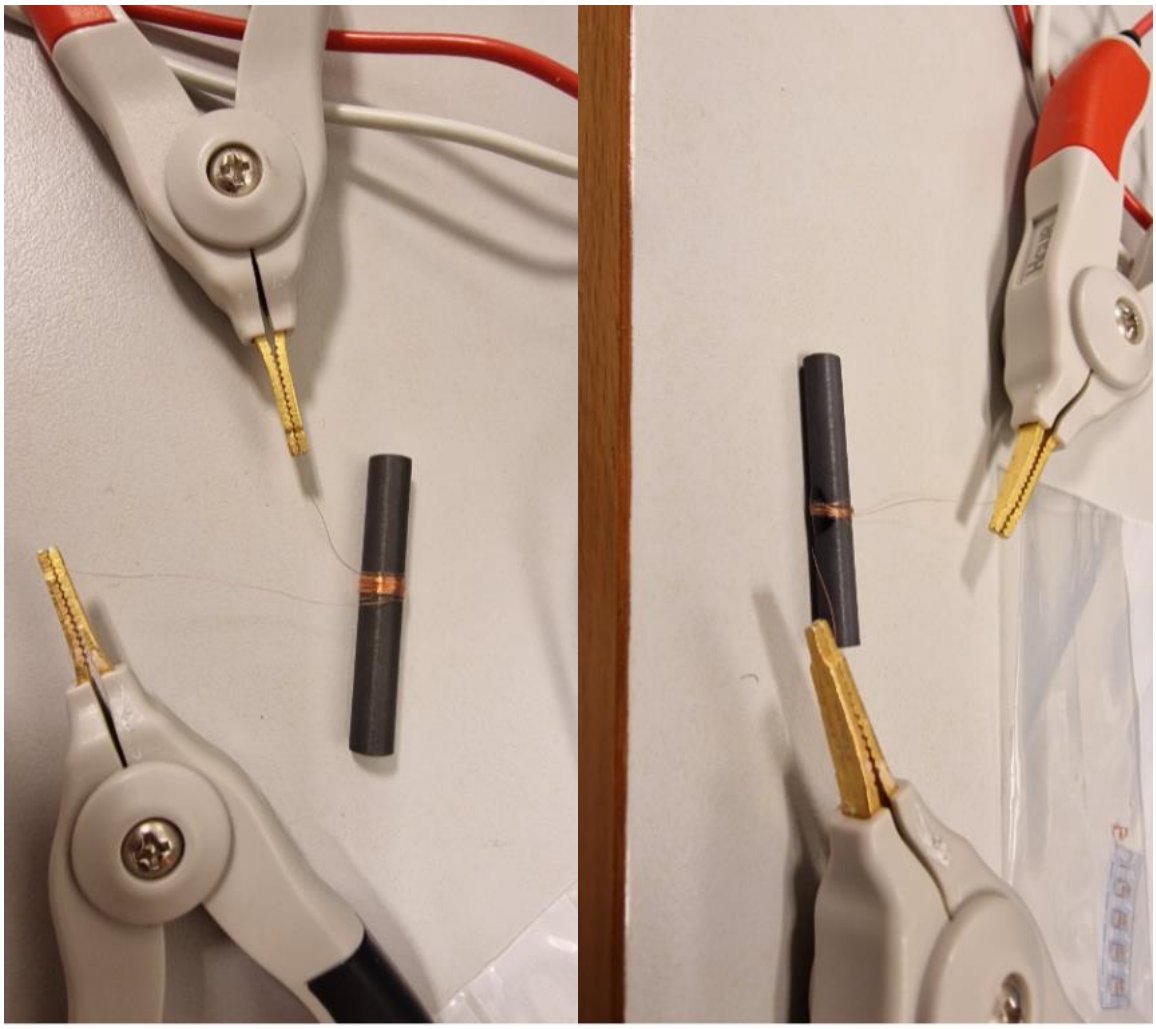

(A) (B)

Figure 5.3: Images of the hand-wound ferrite core coils. (A) Prototype C, Relative permeability = 125, 4 mm diameter, 0.15 mm wire. (B) Prototype D, Relative permeability = 125, 4 mm diameter, 0.07 mm wire.

5.4.3 Measurement method

After construction, the coils were measured to verify the theoretical calculations. Inductance and resistance were measured to check how closely each coil matched the calculated target values. All measurements were performed using a Sourcetronic ST2827A precision LCR meter at 1 kHz and 1 V. The coils were connected with kelvin clip probes to ensure low contact resistance, and short circuit corrections were applied. Both ferrite core and air core reference coils were measured under the same conditions to provide consistent and comparable results.

6. Results

This chapter presents the theoretical and experimental results of the project. The results are shown in tables and graphs to facilitate comparison of different coil configurations.

6.1 Theoretical results of the coils

The theoretical results were calculated using the methods described in Chapter 5. These results include the number of turns, total coil area, DC resistance, magnetic flux, coil Q-factor, and LC magnitude response.

6.1.1 Results for 0.15 mm wire

This section presents the calculated results for coil configurations using a wire diameter of 0.15 mm. Results are presented for different core diameters and core materials. The core materials investigated were air, iron, ferrite nickel-zinc, ferrite manganese-zinc, and Vacuflux 50.

Number of turns

Table 6.1 and figure 6.1 show the calculated number of turns for the different core diameters and core materials.

Table 6.1: Calculated number of turns for different core diameters and core materials using 0.15 mm wire.

Diameter (mm)	Air	Iron	Ferrite (Nickel-Zinc)	Ferrite (Manganese-Zinc)	Vacuflux 50
2	318.30989	31.83099	14.23525	8.21873	5.03292
3	212.20659	21.22066	9.49017	5.47915	3.35528
4	159.15494	15.91549	7.11763	4.10936	2.51646
5	127.32395	12.7324	5.6941	3.28749	2.01317
6	106.1033	10.61033	4.74508	2.73958	1.67764
7	90.94568	9.09457	4.06721	2.34821	1.43798
8	79.57747	7.95775	3.55881	2.05468	1.25823

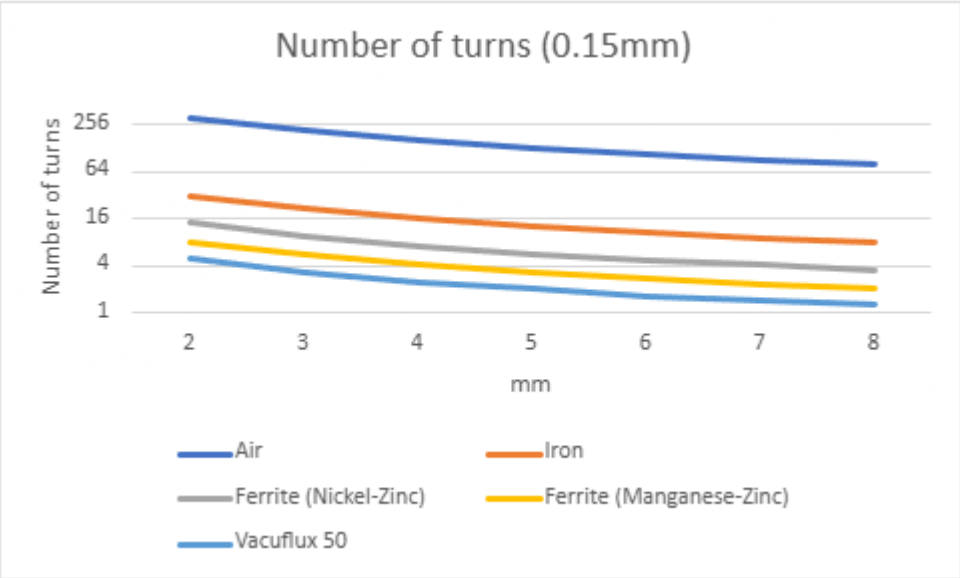

Figure 6.1: Number of turns as a function of core diameter for different core materials using 0.15 mm wire.

Total coil area

Table 6.2 and figure 6.2 show the calculated total coil area of the coil, including both the core and the winding.

Table 6.2: Calculated total coil area for different core diameters and core materials using 0.15 mm wire.

Diameter (mm)	Air	Iron	Ferrite (Nickel-Zinc)	Ferrite (Manganese-Zinc)	Vacuflux 50
2	27.34	5.3092	4.1548	4.1548	4.1548
3	25.52	8.553	8.553	8.553	8.553
4	29.25	14.52	14.52	14.52	14.52
5	33.18	22.06	22.06	22.06	22.06
6	41.79	31.172	31.172	31.172	31.172
7	52.81	41.854	41.854	41.854	41.854
8	66.476	54.106	54.106	54.106	54.106

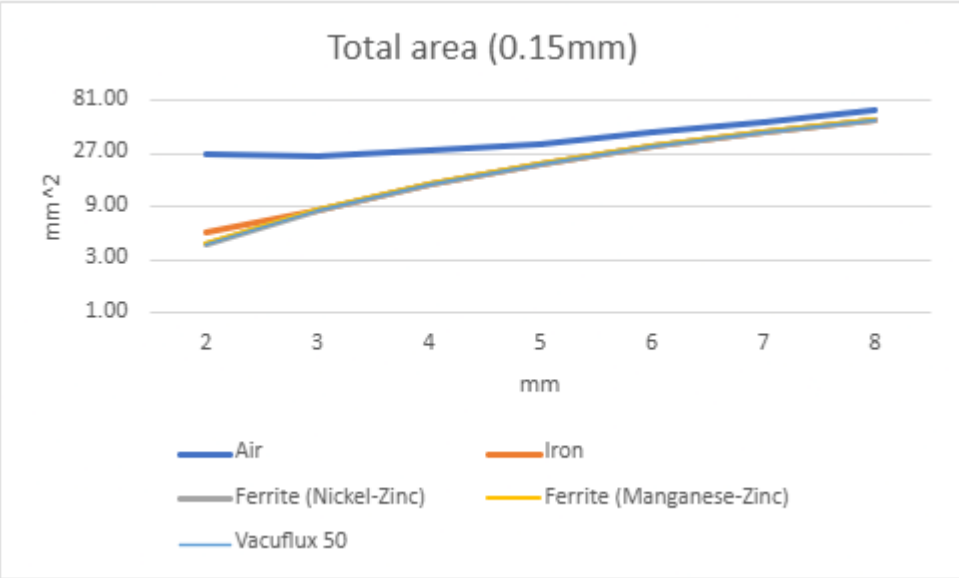

Figure 6.2: Total coil area as a function of core diameter for different core materials using 0.15 mm wire.

DC Resistance

Table 6.3 and figure 6.3 show the calculated DC resistance for the different core materials.

Table 6.3: Calculated DC resistance for different core materials using 0.15 mm wire.

Permeability	Material	DC Resistance
1	Air	2.1792
100	Iron	0.19561
500	Ferrite (Nickel-Zinc)	0.087479
1500	Ferrite (Manganese-Zinc)	0.050506
4000	Vacuflux 50	0.030928

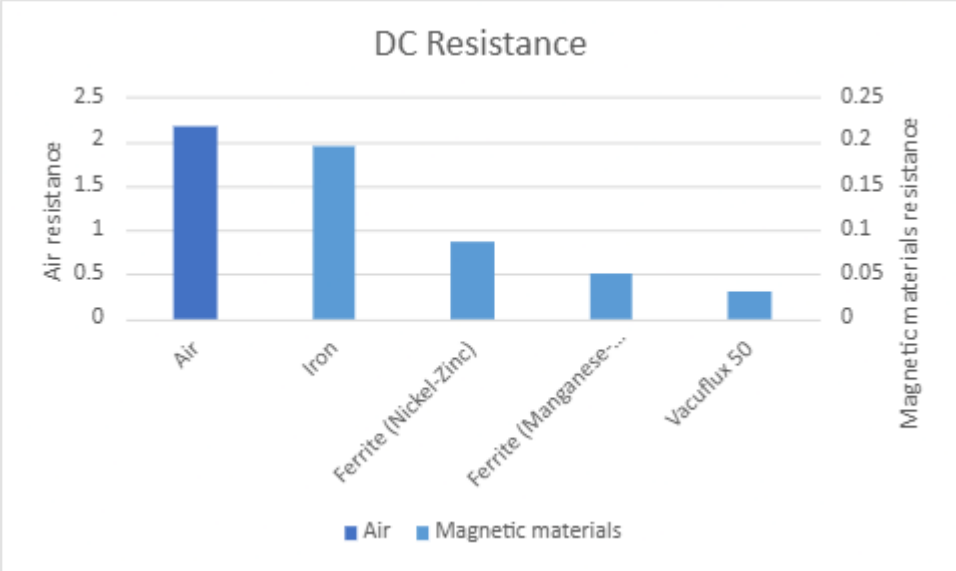

Figure 6.3: DC resistance for different core materials using 0.15 mm wire.

Coil Q-factor

Figure 6.4 show the calculated Q-factor of the coil for the different core diameters and core materials.

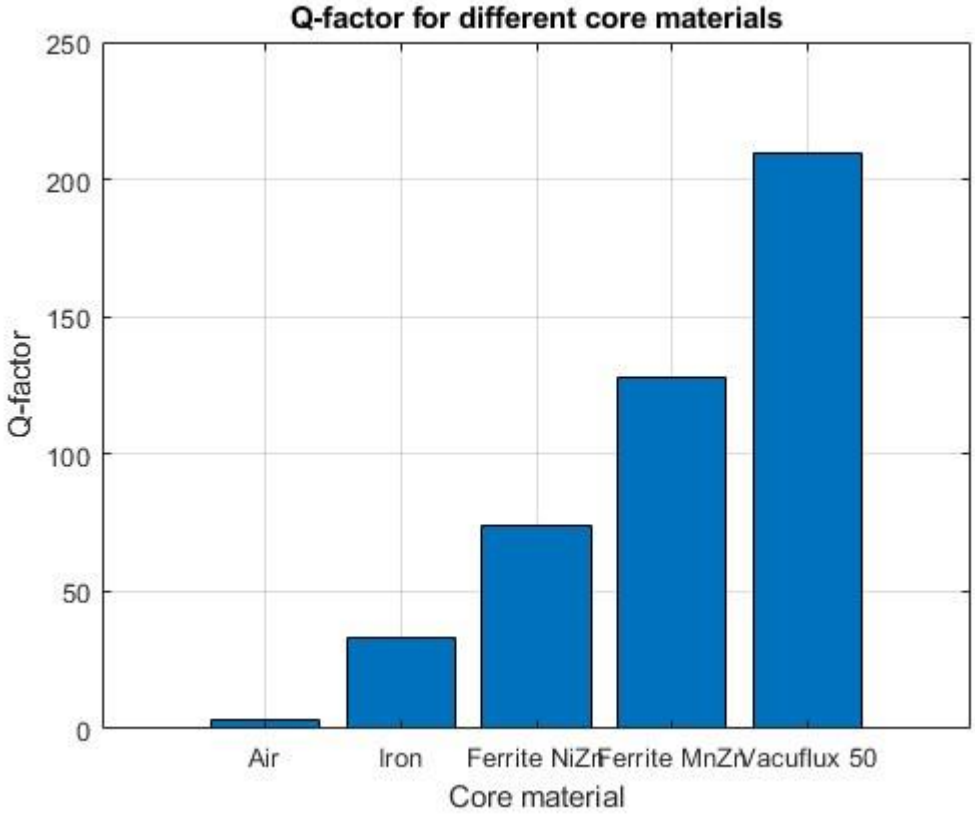

Figure 6.4: Coil Q-factor as a function of core diameter for different core materials using 0.15 mm wire.

LC magnitude response

Figure 6.5 show the magnitude response of the LC circuit when the coil is connected with a

capacitor.

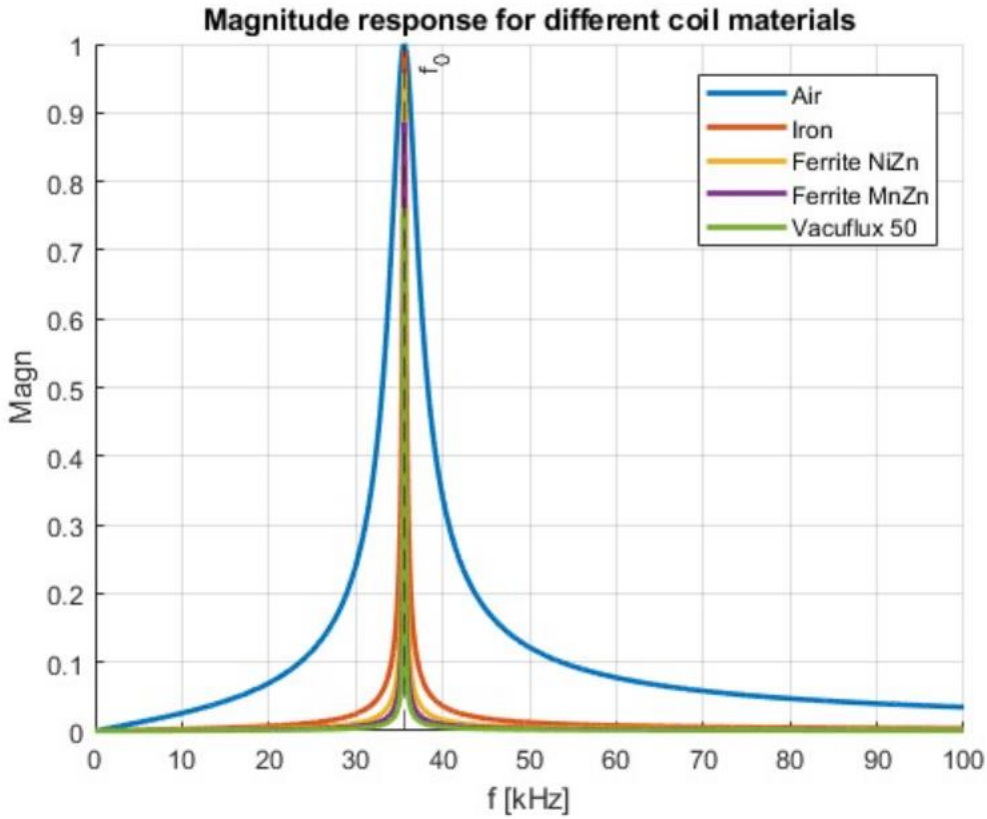

Figure 6.5: Magnitude response of the LC circuit with capacitor for different core materials using 0.15 mm wire

6.1.2 Results for 0.07 mm wire

This section presents the calculated results for coil configurations using a wire diameter of 0.07 mm. The results are presented for different core diameters and core materials. The core materials investigated were the same as for 0.15 mm wire.

Number of turns

Table 6.4 and figure 6.6 show the calculated number of turns for the different core diameters and core materials.

Table 6.4: Calculated number of turns for different core diameters and core materials using 0.07 mm wire.

Diameter (mm)	Air	Iron	Ferrite (Nickel-Zinc)	Ferrite (Manganese-Zinc)	Vacuflux 50
2	318.30989	31.83099	14.23525	8.21873	5.03292
3	212.20659	21.22066	9.49017	5.47915	3.35528
4	159.15494	15.91549	7.11763	4.10936	2.51646
5	127.32395	12.7324	5.6941	3.28749	2.01317
6	106.1033	10.61033	4.74508	2.73958	1.67764
7	90.94568	9.09457	4.06721	2.34821	1.43798
8	79.57747	7.95775	3.55881	2.05468	1.25823

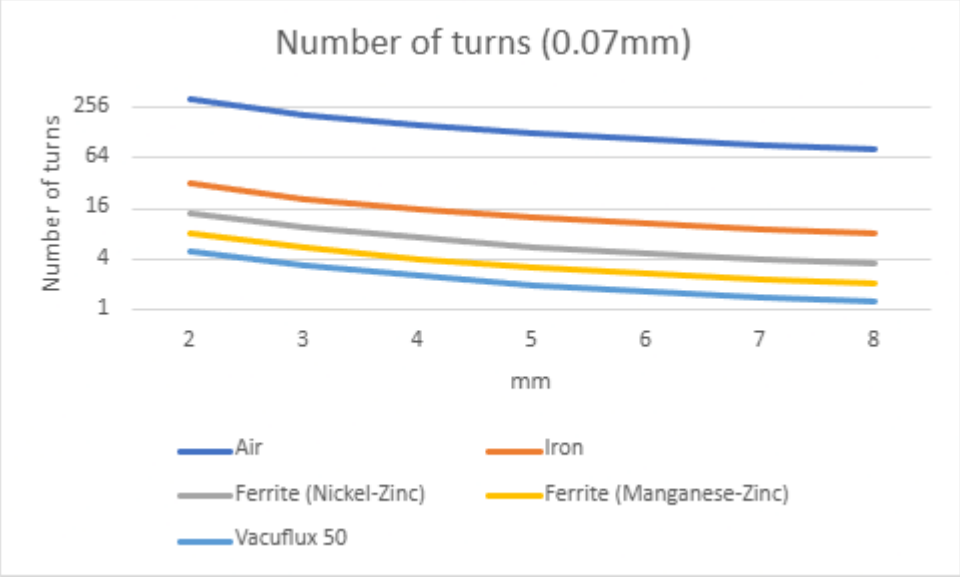

Figure 6.6: Number of turns as a function of core diameter for different core materials using 0.07 mm wire.

Total coil area

Table 6.5 and figure 6.7 show the calculated total coil area of the coil, including both the core and the winding.

Table 6.5: Calculated total coil area for different core diameters and core materials using 0.07 mm wire.

Diameter (mm)	Air	Iron	Ferrite (Nickel-Zinc)	Ferrite (Manganese-Zinc)	Vacuflux 50
2	6.3347	3.5968	3.5968	3.5968	3.5968
3	9.9538	7.7437	7.7437	7.7437	7.7437
4	15.344	13.461	13.461	13.461	13.461
5	23.072	20.75	20.75	20.75	20.75
6	30.975	29.6	29.6	29.6	29.6
7	41.625	40.039	40.039	40.039	40.039
8	53.846	52.04	52.04	52.04	52.04

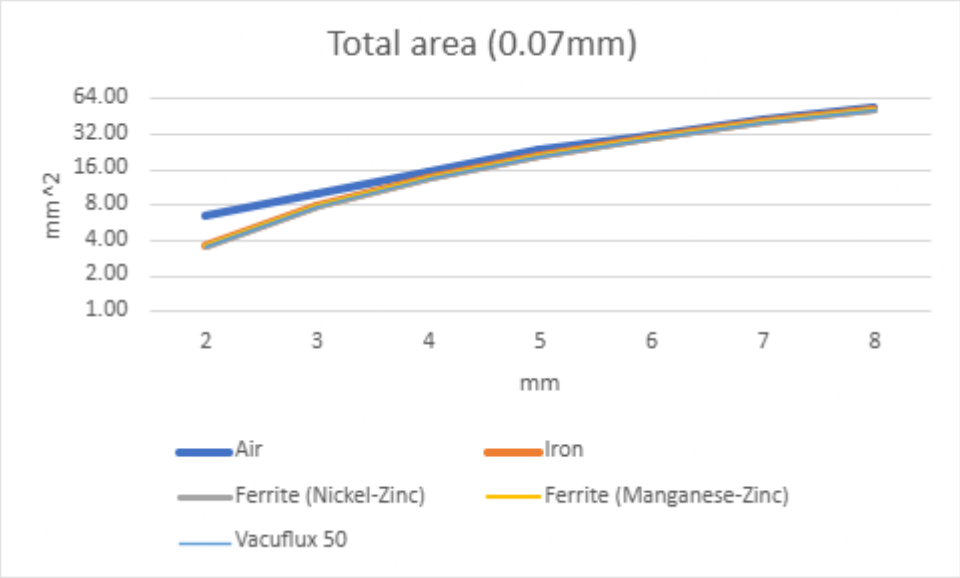

Figure 6.7: Total coil area as a function of core diameter for different core materials using 0.07 mm wire.

DC Resistance

Table 6.6 and figure 6.8 show the calculated DC resistance for the different core materials.

Table 6.6: Calculated DC resistance for different core materials using 0.07 mm wire.

Permeability	Material	DC Resistance
1	Air	9.0029
100	Iron	0.88425
500	Ferrite (Nickel-Zinc)	0.39545
1500	Ferrite (Manganese-Zinc)	0.22831
4000	Vacuflux 50	0.13981

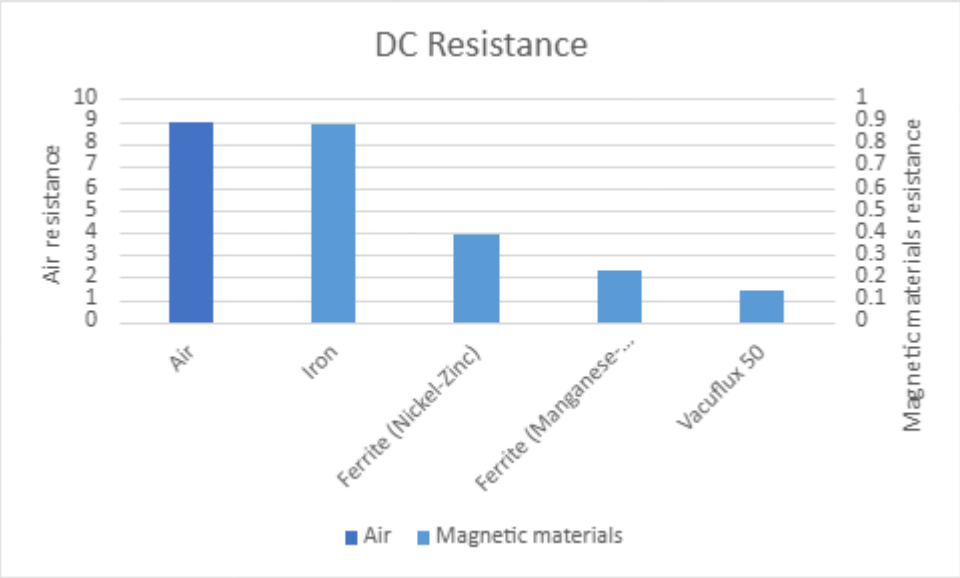

Figure 6.8: DC resistance for different core materials using 0.07 mm wire.

Coil Q-factor

Figure 6.9 show the calculated Q-factor of the coil for the different core diameters and core materials.

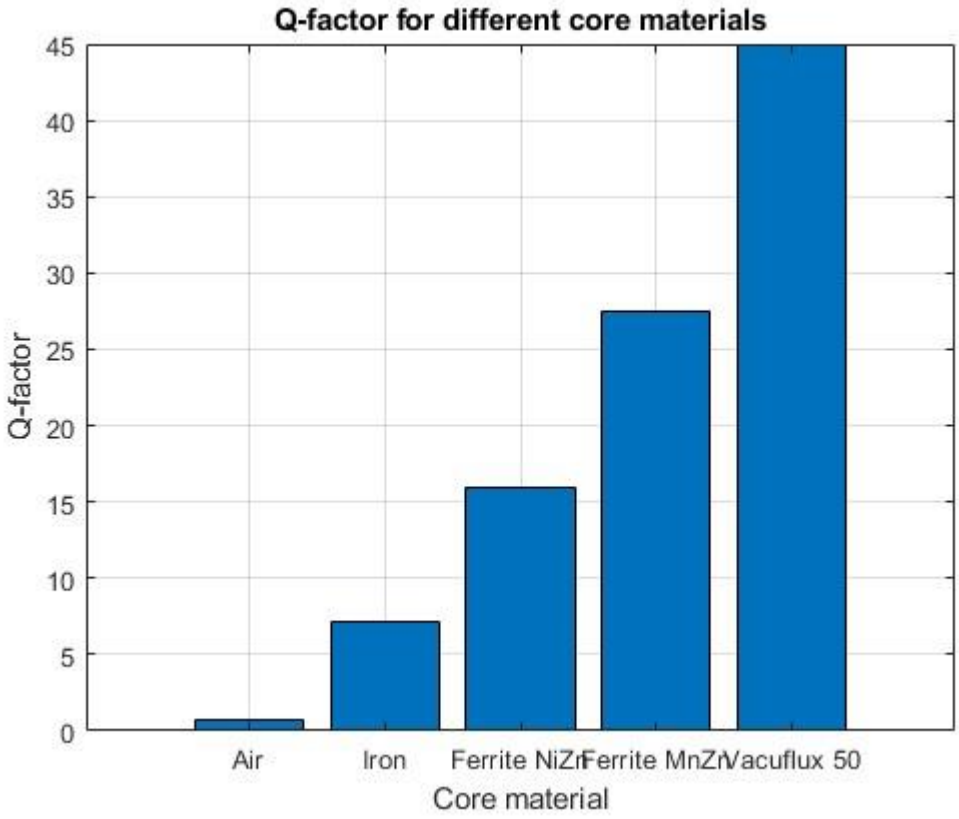

Figure 6.9: Coil Q-factor as a function of core diameter for different core materials using 0.07 mm wire.

LC magnitude response

Figure 6.10 show the magnitude response of the LC circuit when the coil is connected with a capacitor.

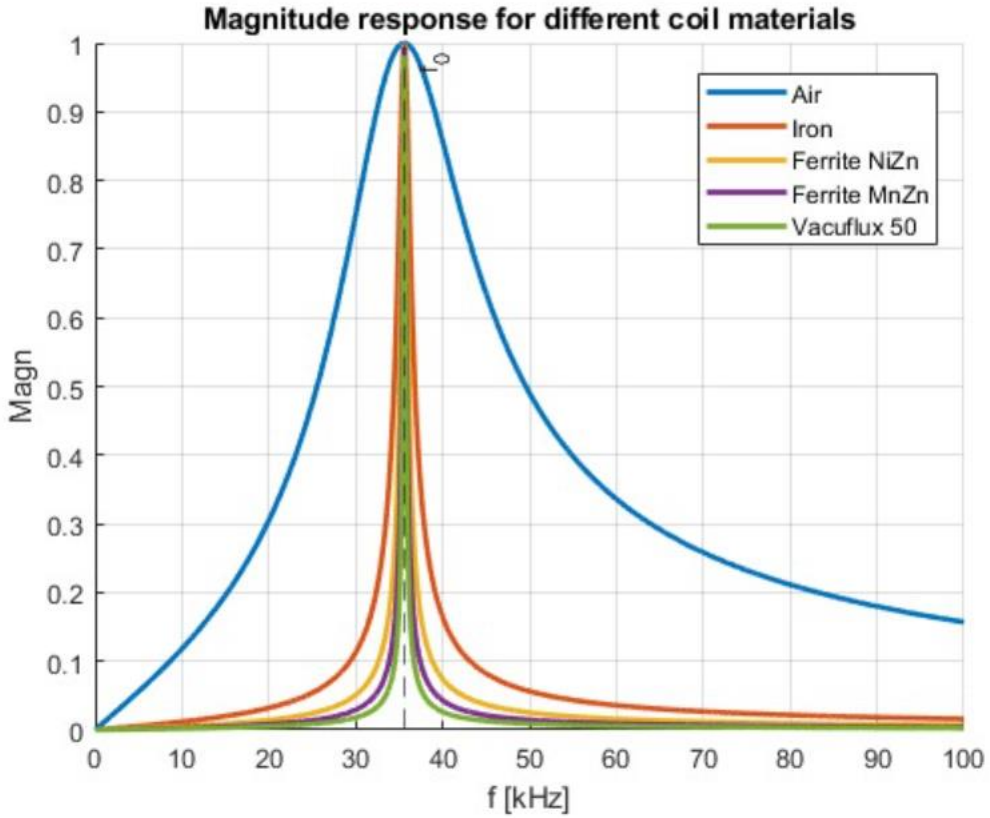

Figure 6.10: Magnitude response of the LC circuit with capacitor for different core materials using 0.07 mm wire

6.1.3 Magnetic flux

Figure 6.11 shows a schematic illustration of the magnetic flux Φ as a function of the square of the core diameter (d^2) for different relative permeabilities. The curves start from zero and increase toward the target flux Φ_T, illustrating that higher permeability cores achieve the target flux at smaller diameters, while lower permeability cores require larger diameters.

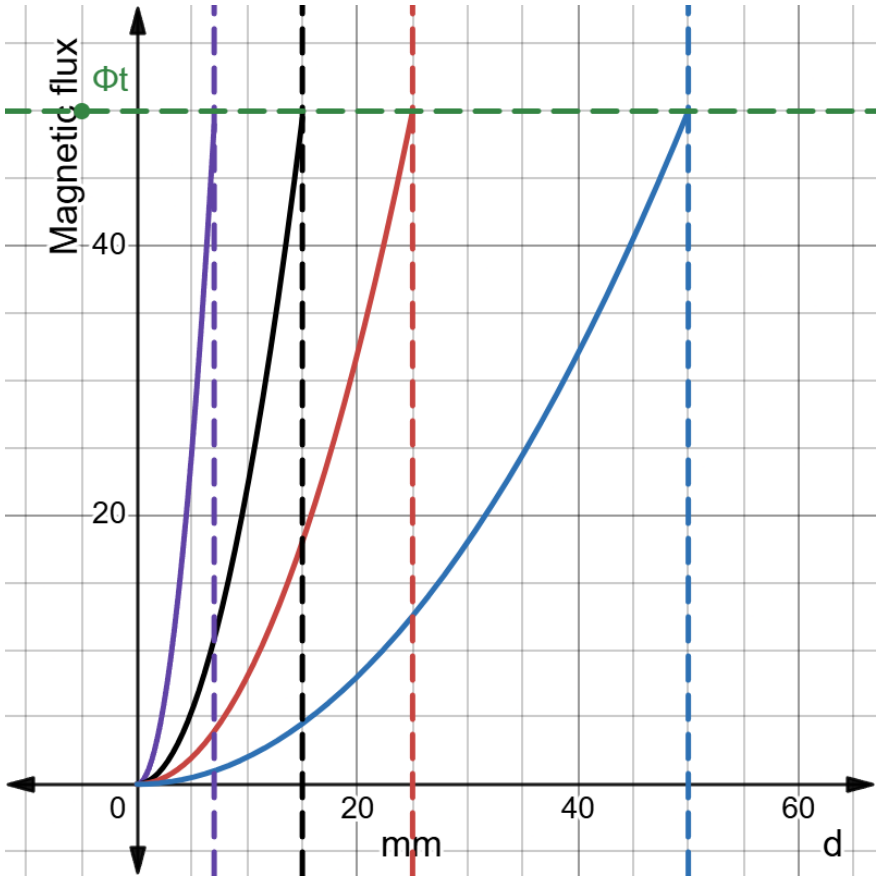

Figure 6.11: Schematic illustration of magnetic flux in cores with different relative permeabilities. The horizontal dashed line indicates the target flux Φ_T. Colors represent relative permeability, with the leftmost curve having the highest permeability and the rightmost curve the lowest.

6.2 Results from the experimental coils

The experimental measurements were performed at Oticon Medical's laboratory at a test frequency of 1 kHz with a signal level of 1 V using the Sourcetronic ST2827A precision LCR meter.

6.2.1 Hand-Wound Prototype Coils

Four prototype coils were constructed by hand on two ferrite rod cores. Two coils were wound on a 2300 relative permeability rod with a core diameter of 6 mm using 3 turns, one with 0.15 mm wire (Prototype A) and one with 0.07 mm wire (Prototype B). The remaining two coils were wound on a 125 relative permeability rod with a core diameter of 4 mm using 15 turns, again with 0.15 mm wire (Prototype C) and 0.07 mm wire (Prototype D). The measured results are presented in table 6.7.

Table 6.7: Measured results for hand-wound prototype coils (1 kHz / 1 V)

Prototype	Relative permeability	Core diameter (mm)	Wire diameter (mm)	Number of turns	Measured inductance (µH)	Measured resistance (Ω)
A	2300	6	0.15	3	0.8	0.05
B	2300	6	0.07	3	0.8	0.66
C	125	4	0.15	14	6.8	0.25
D	125	4	0.07	14	6.8	1.77

6.2.2 Prebuilt Reference Inductors

Three prebuilt inductors were measured under the same conditions to verify the measurement setup and provide a comparison baseline. The results are presented in table 6.8.

Table 6.8: Measured results for prebuilt reference inductors (1 kHz / 1 V)

Coil	Core type	Inductance (µH)	Resistance (Ω)
1	Air	106	2.85
2	Ferrite	10	0.54
3	ceramic	0.1	0.28

7. Discussion

This chapter analyses the results from the calculations and measurements. The discussion is divided into three main parts: first, the theoretical relationships between coil parameters and their effect on inductor performance; second, a comparison between the constructed prototypes and the theoretical predictions, including an explanation of the observed discrepancies; and third, the implications of these findings for hearing implant applications.

7.1 Theoretical parameter relationships

7.1.1 Effect of core material

The core material is one of the most important parameters affecting the inductance of a coil. A material with higher relative permeability increases the inductance for a given number of turns. This means that fewer turns are needed to reach the same target inductance when a high-permeability core is used compared with an air core.
The theoretical results show that increasing the relative permeability greatly reduces the required number of turns. Since the wire length depends on the number of turns, fewer turns also result in shorter total wire length. This reduces the DC resistance of the coil and improves the Q-factor.
A low-permeability material, such as air, requires more turns to reach the same inductance. This increases both the total wire length and the resistance. Therefore, the results show a clear trade-off between core material and coil geometry: a high-permeability core allows a smaller and less resistive coil, while a low-permeability core requires a larger winding to reach the same inductance.

7.1.2 Effect of wire diameter

The wire diameter mainly affects the DC resistance of the coil. A larger wire diameter gives a larger cross-sectional area, which allows current to flow with lower resistance. The results show that the 0.15 mm wire gives significantly lower resistance than the 0.07 mm wire.
However, increasing the wire diameter also increases the physical size of the winding. This means that a thicker wire improves the electrical performance by lowering resistance, but it also increases the total coil dimensions. A thinner wire allows a more compact winding, but results in higher resistance and lower Q-factor.
The results therefore show that wire diameter creates a trade-off between resistance and coil size. A thicker wire is better for reducing losses, while a thinner wire is better when the winding must be physically smaller.

7.1.3 Effect of operating frequency and Q-factor

The operating frequency has a strong influence on the coil behavior. The Q-factor describes the relationship between the inductive reactance and the resistance of the coil. When the frequency increases, the inductive reactance also increases, which generally increases the Q-factor if the inductance and resistance remain constant.
At lower frequencies, the inductive reactance is small compared with the winding resistance. This gives a lower Q-factor and means that the coil behavior is more dominated by resistance. At higher frequencies, the inductive reactance becomes larger, which gives a higher Q-factor and a stronger inductive behavior.
The results show that resistance, inductance, and frequency are closely connected. A coil with lower resistance or higher inductance will generally have a higher Q-factor. Therefore,

increasing the permeability, reducing the number of turns, or using a thicker wire can improve the Q-factor by reducing the winding resistance.

7.1.4 LC circuit and bandwidth

When the coil is connected with a capacitor, an LC circuit is formed. The circuit has a resonance frequency that depends on the inductance and capacitance. A higher inductance or capacitance gives a lower resonance frequency, while a lower inductance or capacitance gives a higher resonance frequency.
The results show that changing the coil geometry affects the LC response. If the core material or number of turns increases the inductance, the resonance frequency shifts downward. If the inductance is reduced, the resonance frequency shifts upward. This means that the coil geometry directly affects where the circuit resonates.
The bandwidth is connected to the Q-factor. A higher Q-factor gives a narrower bandwidth and a sharper resonance peak. A lower Q-factor gives a wider bandwidth and a flatter resonance response. Since resistance lowers the Q-factor, coils with higher DC resistance give a broader and less selective LC response.
Therefore, the LC results show that inductance, resistance, resonance frequency, Q-factor, and bandwidth are all connected. Changing one coil parameter affects the full circuit response.

7.1.5 Magnetic flux

The magnetic flux results show how core diameter and relative permeability affect the flux in the core. A higher relative permeability allows the same magnetic flux to be reached with a smaller core diameter. A lower relative permeability requires a larger core diameter to reach the same flux.
This means that permeability and core size can compensate for each other. A high-permeability material can achieve the required flux with a smaller core area, while a low-permeability material needs a larger core area. Therefore, increasing the permeability can reduce the required core size.
Figure 6.11 illustrates this relationship. The curves with higher relative permeability reach the target flux at a smaller value of core diameter squared. The curves with lower relative permeability reach the target flux later, meaning that a larger core diameter is required.
The results show that magnetic flux is strongly affected by both material choice and core geometry. To achieve the same flux, a designer can either increase the relative permeability or increase the core diameter.

7.2 Constructed Prototypes: comparison with theory

7.2.1 Observed discrepancies

When the hand-wound ferrite core prototypes were measured, the results differed substantially from the theoretical predictions. The coil wound on the 2300 relative permeability rod with 3 turns measured at approximately 0.8 μH, against a predicted value of 180 μH. The coil wound on the 125 relative permeability rod with 14 turns measured approximately 6.8 μH, against a predicted 97 μH. When back calculating the effective relative permeability from the measured inductance and the known geometry it gave a value of approximately 9 and 11, more than two orders of magnitude below the datasheet specifications.

7.2.2 Why the results did not match

The fact that two different cores from two different material lots produced almost the same back calculated effective relative permeability of approximately 9 - 11 strongly suggests a systematic effect rather than a construction defect or measurement error. Several hypotheses were considered.

The first hypothesis was that the construction itself was at fault, for example, insufficient coupling between the winding and the core, or a winding length too short relative to the total core length. This was tested by breaking the ferrite rod in half and remeasuring the prototype. The measured inductance was essentially unchanged, confirming that the effective inductance depends on the section of core covered by the winding, not on the total rod length. This ruled out the construction as the primary cause.

Another possible explanation was that the measurement setup itself was incorrect, for example due to calibration errors, poor contact, or an incorrect measurement method. However, this explanation was rejected after measuring the prebuilt reference inductors. These inductors had known nominal values and were measured close to their specified values. This confirmed that the LCR meter, the Kelvin clip connection, and the general measurement procedure were working correctly.

The MATLAB code and theoretical calculations were also checked. This was done by applying the same calculation method to a prebuilt air-core inductor with known properties. The calculated value agreed with the measured and expected inductance of the air-core coil. This confirmed that the code, formulas, and calculation method were correct when the input parameters were accurate.

After further analysis together with the examiner and supervisor, the most likely explanation for the low measured permeability was that the effective permeability of the ferrite cores under the actual measurement conditions was much lower than the nominal datasheet values. Ferrite materials can have permeability values that depend on the specified measurement conditions, and the nominal values in datasheets cannot always be applied directly to a practical coil design.
The prototypes were first measured at 1 kHz. Additional measurements were also performed at higher frequencies, up to 300 kHz, which was the upper limit of the available measurement setup. However, the measured inductance did not change significantly over this frequency range. This indicates that the low inductance was not caused by a small frequency variation within the tested range, but rather by the fact that the effective permeability of the ferrite cores was much lower than the nominal datasheet values under the measurement conditions used.
This conclusion is supported by the rebuild experiment described in the next section. When the back-calculated effective permeability was used as the design input in MATLAB, the predicted inductance matched the measured value to within 3 %. This confirms that the model is reliable when the correct effective permeability is used, and that the discrepancy was mainly caused by the material's effective permeability under the actual measurement conditions rather than by the measurement setup or the construction.

7.2.3 Verification and rebuild

To confirm that the model and measurement procedure were internally consistent, a rebuild was carried out. Using the back calculated effective relative permeability of 11 as the design input, MATLAB predicted that 32 turns on the 2300 relative permeability rod would yield 109 µH. The measured value was 106.4 µH within 3% of the prediction. This confirms that the discrepancy is reproducible and predictable, and that the MATLAB model is reliable once the correct effective permeability is used.

The three pre-built reference inductors for the study with nominal values of 100 µH, 10 µH, and 100 nH all measured within a few percent of their specified values. This independently validates the LCR meter setup, the Kelvin clip probing technique, and the measurement procedure. Taken together with the successful rebuild, the validation chain isolates the discrepancy to the magnetic behavior of the ferrite material at the LCR meter's signal level, and not to the measurement setup, the model, or the construction process.

7.3 Implications for hearing Implant applications

The results have several important implications for hearing implant applications. In this type of application, the coil must be compact, efficient, and safe to use close to biological tissue. Therefore, the choice of core material, wire diameter, number of turns, and total coil size becomes especially important.

A high-permeability core is beneficial because it can reach the required inductance with fewer turns. This reduces the total wire length, lowers the DC resistance, and makes the coil more compact. Lower resistance also reduces power losses and heat generation, which is important in implantable devices.

However, high-permeability magnetic materials may interact with external magnetic fields, for example during medical imaging. This means that the material choice must also consider magnetic compatibility. Air cores or low-permeability materials are more stable in external magnetic fields, but they require more turns or a larger core diameter to reach the same inductance or magnetic flux. This usually increases both coil size and resistance.

The wire diameter also has practical importance. A thicker wire reduces resistance and heat losses, but it increases the winding size. A thinner wire makes the winding smaller, but increases resistance. Therefore, the wire diameter must be chosen as a balance between compactness and efficiency.

The LC circuit behaviour is also important because the coil will operate as part of a complete electrical system. The inductance, capacitance, resistance, Q-factor, resonance frequency, and bandwidth must be matched to the system requirements. A coil with too high resistance may give a weaker resonance response and lower efficiency.

Overall, the final coil design for a hearing implant must balance several requirements: small size, low resistance, sufficient inductance, suitable magnetic flux, acceptable bandwidth, low heat generation, and magnetic compatibility. The results show that there is no single best coil design. Instead, the best solution depends on the specific requirements of the implant system.

8. Conclusion

This thesis investigated how core material, core diameter, wire diameter, and number of turns affect wire-wound inductors for implantable hearing devices. A MATLAB-based model was combined with prototype construction and measurements at Oticon Medical.
The theoretical results showed that higher relative permeability reduces the number of turns needed to reach a target inductance. This also reduces wire length and DC resistance, which improves compactness and efficiency. A thicker wire gave lower resistance than a thinner wire, but increased the total coil size. The results also showed that high permeability materials can achieve the same magnetic flux with a smaller core diameter.
The LC circuit analysis showed that the coil must be designed together with the capacitor and the rest of the circuit. Inductance, resistance, Q-factor, resonance frequency, and bandwidth all affect the final performance.
The experimental results showed that the lower-than-expected inductance was mainly caused by the frequency dependence of the ferrite cores. The nominal datasheet permeability values did not represent the effective permeability at the 1 kHz measurement frequency, which led to much lower inductance than predicted.
Other possible explanations were considered but were not found to be the main cause. The core length, measurement setup, and MATLAB model were checked through additional measurements and reference inductors. These checks supported the conclusion that the discrepancy was mainly due to the ferrite material behavior at the measurement frequency.
Therefore, future coil designs should not rely directly on nominal datasheet permeability values. Instead, material data should be verified at the intended operating frequency, while also balancing inductance, resistance, size, bandwidth, heat generation, and magnetic compatibility.

Future work and recommendations for Oticon Medical

This thesis can be used by Oticon Medical as a basis for making faster design decisions for future inductor designs. The MATLAB model makes it possible to quickly compare different core materials, core diameters, wire diameters, and number of turns before building physical prototypes.
By using the model, Oticon Medical can estimate what is required to reach a target inductance, resistance, Q-factor, resonance frequency, and bandwidth. This can reduce trial-and-error work and help identify which coil designs are worth testing further.

References

[1] B. C. J. Moore, An Introduction to the Psychology of Hearing, 6th ed. Leiden, Netherlands: Brill, 2012. Available: https://web.uvic.ca/~aschloss/course_mat/MUS%20511/articles/An%20Introduction%20to%20the%20Psychology%20of%20Hearing%20by%20Brian%20Moore%206th%20Edition.pdf
[2] F. Bhatt et al., "Advanced Management of Hearing Loss: A Comprehensive Review," J. Clin. Med., Dec. 2024. [Online]. Available: https://www.mdpi.com/2077-0383/13/23/7409
[3] M. Ghovanloo and K. Najafi, "A wide-band frequency-shift keying wireless link for inductively powered biomedical implants," IEEE Trans. Circuits Syst. I, Dec. 2004. Available: https://www.researchgate.net/publication/3450876_A_Wideband_Frequency-Shift_Keying_Wireless_Link_for_Inductively_Powered_Biomedical_Implants
[4] U. M. Jow and M. Ghovanloo, "Design and optimization of printed spiral coils for efficient transcutaneous inductive power transmission," IEEE Trans. Biomed. Circuits Syst., Sep. 2007. Available: https://www.researchgate.net/publication/3481287_Design_and_Optimization_of_Printed_Spiral_Coils_for_Efficient_Transcutaneous_Inductive_Power_Transmission
[5] Oticon Medical, "About Oticon Medical," oticonmedical.com. [Online]. Available: https://www.oticonmedical.com/en-GB [Accessed: March 2026].
[6] W. H. Hayt and J. A. Buck, Engineering Electromagnetics, 8th ed. New York, NY, USA: McGraw-Hill, 2012. Available: http://www.uop.edu.pk/ocontents/EMT.pdf
[7] R. W. Erickson and D. Maksimovic, Fundamentals of Power Electronics, 3rd ed. Cham, Switzerland: Springer, 2020. Available: https://fmipa.umri.ac.id/wp-content/uploads/2016/03/R._Erickson_Fundamentals_of_Power_Electronics_pBookZZ.org_.pdf
[8] C. Bowick, RF Circuit Design, 2nd ed. Burlington, MA, USA: Newnes, 2008. Available: https://ia601604.us.archive.org/21/items/RFCircuitDesign2ndEdition/RF%20Circuit%20Design%20-%202nd%20Edition.pdf

Appendices

```
clear;
clc;
close all;
%% ===================== GIVEN CONSTANTS =====================
% Target inductance of the coil
L = 100e-6; % Inductance [H]
% Magnetic permeability of free space
mu0 = 4*pi*1e-7; % Permeability [H/m]
% Core dimensions
D_core = 0.005; % Core diameter [m]
l_coil = 0.004; % Coil length [m]
% Copper wire properties
rho = 1.678e-8; % Copper resistivity [Ohm*m]
D_wire = 0.00007; % Wire diameter [m]
% Operating conditions
f = 10000; % Operating frequency [Hz]
Psi = 1; % Proximity effect factor [-]
% Capacitor used for the RLC resonance calculation
C = 200e-9; % Capacitance [F]
%% ===================== MATERIALS =====================
% List of core materials to compare
materials = {'Air', 'Iron', 'Ferrite NiZn', 'Ferrite MnZn', 'Vacuflux 50'};
% Relative permeability values for each material above
mur_values = [1, 100, 500, 1500, 4000];
%% ===================== GEOMETRY =====================
% Convert diameters to radii
R_core = D_core/2; % Core radius [m]
R_wire = D_wire/2; % Wire radius [m]
% Cross-sectional areas of the core and wire
A_core = pi*R_core^2; % Core cross-sectional area [m^2]
A_wire = pi*R_wire^2; % Wire cross-sectional area [m^2]
%% ===================== STORAGE FOR RESULTS =====================
% Preallocate arrays to store calculated values for each material
N_values = zeros(1, length(materials)); % Number of turns
l_wire_values = zeros(1, length(materials)); % Total wire length [m]
DCR_values = zeros(1, length(materials)); % DC resistance [Ohm]
ACR_values = zeros(1, length(materials)); % AC resistance [Ohm]
XL_values = zeros(1, length(materials)); % Inductive reactance [Ohm]
Q_values = zeros(1, length(materials)); % Coil quality factor
A_total_values = zeros(1, length(materials)); % Total coil area [m^2]
D_outer_values = zeros(1, length(materials)); % Outer coil diameter [m]
R_outer_values = zeros(1, length(materials)); % Outer coil radius [m]
layers_values = zeros(1, length(materials)); % Number of winding layers
%% ===================== CALCULATIONS FOR EACH MATERIAL =====================
for k = 1:length(materials)
% Get the relative permeability for the current material
mur = mur_values(k);
% Calculate the absolute permeability of the core material
mu_core = mu0*mur;
% Calculate the number of turns required to reach the target inductance
N = sqrt((L*l_coil)/(mu_core*A_core));
% Estimate the total wire length based on the number of turns
l_wire = N*pi*D_core;
% Calculate the DC resistance of the copper wire
DCR = (rho*l_wire)/A_wire;
% Calculate skin depth in copper at the selected frequency
% Since this is a copper wire, mu0 is used instead of core permeability
delta = sqrt(rho/(pi*f*mu0));
```

```
% Estimate the skin effect correction factor
% If the skin depth is smaller than the wire radius, resistance increases
if delta < R_wire
Xi = R_wire/(2*delta);
else
Xi = 1;
end
% Calculate AC resistance including skin and proximity effects
ACR = DCR*Xi*Psi;
% Calculate inductive reactance at the operating frequency
XL = 2*pi*f*L;
% Calculate the coil quality factor
Q = XL/ACR;
% Calculate how many turns fit in one winding layer
turns_per_layer = floor(l_coil/D_wire);
% Calculate the number of layers needed for the winding
number_of_layers = ceil(N/turns_per_layer);
% Calculate the outer diameter and radius of the finished coil
D_outer = D_core + 2*number_of_layers*D_wire;
R_outer = D_outer/2;
% Calculate total cross-sectional area of the coil including windings
A_total = pi*R_outer^2;
% Store all calculated values for the current material
N_values(k) = N;
l_wire_values(k) = l_wire;
DCR_values(k) = DCR;
ACR_values(k) = ACR;
XL_values(k) = XL;
Q_values(k) = Q;
A_total_values(k) = A_total;
D_outer_values(k) = D_outer;
R_outer_values(k) = R_outer;
layers_values(k) = number_of_layers;
end
%% ===================== DISPLAY GENERAL GEOMETRY =====================
fprintf('\n=====================================================\n');
fprintf(' WIRE AND CORE GEOMETRY\n');
fprintf('=====================================================\n');
% Display basic wire dimensions
fprintf('\n--- WIRE GEOMETRY ---\n');
fprintf('Wire radius, R_wire: %.6e m\n', R_wire);
fprintf('Wire diameter, D_wire: %.6e m\n', D_wire);
fprintf('Wire area, A_wire: %.6e m^2\n', A_wire);
% Display basic core dimensions
fprintf('\n--- CORE GEOMETRY ---\n');
fprintf('Core radius, R_core: %.6e m\n', R_core);
fprintf('Core diameter, D_core: %.6e m\n', D_core);
fprintf('Core area, A_core: %.6e m^2\n', A_core);
% Display skin effect parameters
fprintf('\n--- SKIN EFFECT ---\n');
fprintf('Skin depth, delta: %.6e m\n', delta);
fprintf('Skin factor, Xi: %.6f\n', Xi);
fprintf('Proximity factor, Psi: %.6f\n', Psi);
%% ===================== DISPLAY RESULTS TABLE =====================
fprintf('\n=====================================================\n');
fprintf(' COIL RESULTS\n');
fprintf('=====================================================\n');
% Create a table containing all calculated results
Results = table( ...
materials', ...
```

```
mur_values', ...
N_values', ...
l_wire_values', ...
DCR_values', ...
ACR_values', ...
XL_values', ...
Q_values', ...
layers_values', ...
R_outer_values', ...
D_outer_values', ...
A_total_values', ...
'VariableNames', {'Material', 'mur', 'N_turns', 'Wire_length_m', ...
'DCR_Ohm', 'ACR_Ohm', 'XL_Ohm', 'Q_factor', ...
'Number_of_layers', 'R_outer_m', 'D_outer_m', 'A_total_m2'} );
% Display the results table in the MATLAB command window
disp(Results);
%% ==================== RLC RESONANCE VALUES ====================
% Calculate resonance frequency of an ideal LC circuit
f0 = 1/(2*pi*sqrt(L*C)); % Resonance frequency [Hz]
% Convert resonance frequency to angular frequency
w0 = 2*pi*f0; % Angular resonance frequency [rad/s]
fprintf('\n=====================================================\n');
fprintf(' RLC RESONANCE\n');
fprintf('=====================================================\n');
% Display resonance information
fprintf('Capacitance, C: %.6e F\n', C);
fprintf('Resonance frequency, f0: %.2f Hz\n', f0);
fprintf('Resonance frequency, f0: %.2f kHz\n', f0/1000);
%% ==================== RLC Q-FACTOR FOR EACH COIL ====================
% Calculate the RLC quality factor for each material
Q_RLC_values = (w0*L)./ACR_values;
fprintf('\n--- RLC Q-FACTOR FOR EACH MATERIAL ---\n');
% Print one RLC Q-factor value per material
for k = 1:length(materials)
fprintf('%s: Q_RLC = %.4f\n', materials{k}, Q_RLC_values(k));
end
%% ==================== Q-FACTOR BAR GRAPH ====================
% Bar chart showing coil Q-factor for each core material
figure;
bar(Q_values);
grid on;
set(gca, 'XTickLabel', materials);
xlabel('Core material');
ylabel('Q-factor');
title('Q-factor for different core materials');
%% ==================== RLC MAGNITUDE RESPONSE GRAPH ====================
% Frequency range used for plotting the resonance curve
f_graph = linspace(0, 100e3, 2000);
% Normalize frequency with respect to resonance frequency
x = f_graph/f0;
figure;
hold on;
% Plot normalized magnitude response for each material
for k = 1:length(materials)
% Use the RLC Q-factor for the current material
Q_real = Q_RLC_values(k);
% Normalized magnitude response of a series RLC circuit
Magn = (x./Q_real) ./ sqrt((1 - x.^2).^2 + (x./Q_real).^2);
% Plot magnitude response in kHz
plot(f_graph/1000, Magn, 'LineWidth', 2);
```

```
end
% Mark the resonance frequency
xline(f0/1000, '--', 'f_0');
grid on;
xlabel('Frequency [kHz]');
ylabel('Magnitude');
title('Magnitude response for different coil materials');
legend(materials, 'Location', 'best');
%% ===================== DCR GRAPH =====================
% Bar chart showing DC resistance for each material
figure;
bar(DCR_values);
grid on;
set(gca, 'XTickLabel', materials);
xlabel('Core material');
ylabel('DCR [Ohm]');
title('DC resistance for different core materials');
%% ===================== NUMBER OF TURNS GRAPH =====================
% Bar chart showing required number of turns for each material
figure;
bar(N_values);
grid on;
set(gca, 'XTickLabel', materials);
xlabel('Core material');
ylabel('Number of turns');
title('Number of turns for different core materials');
```